Ellipsometric configurations using a phase retarder and a rotating polarizer and analyzer at any speed ratio

Sofyan A. Taya†, Taher M. El-Agez, and Anas A. Alkanoo

Physics Department, Islamic University of Gaza, P.O. Box 108, Gaza, Palestinian Authority

(Received 22 May 2012)

In this paper, we propose an ellipsometer using a phase retarder and rotating polarizer and analyzer at a speed ratio 1:N. Different ellipsometric configurations are presented by assuming $N = 1$, 2, and 3. Moreover, two values of the offset angle of the retarder are considered for each ellipsometric configuration. The Mueller formalism is employed to extract the Stokes parameters, from which the intensity received by the detector is obtained. The optical properties of c-Si are calculated using all configurations. A comparison between different configurations is carried out considering the effect of the noise on the results and the uncertainties in the ellipsometric parameters as functions of the uncertainties of the Fourier coefficients. It is found that the alignment of the phase retarder has a crucial impact on the results and the ellipsometric configuration with speed ratio 1:1 is preferred over the other configurations.

Keywords: ellipsometry, phase retarder, rotating polarizer and analyzer

PACS: 07.60.Fs **DOI:** 10.1088/1674-1056/21/11/110701

1. Introduction

Ellipsometry[1−5] is a well-established technique used to study the optical properties of many kinds of materials. The reflection from a sample is characterized by two ellipsometric angles ψ and Δ, which are defined as[1]

$$\tan\psi = \frac{|r_{\rm p}|}{|r_{\rm s}|}, \tag{1}$$

and

$$\Delta = \arg\frac{r_{\rm p}}{r_{\rm s}}, \tag{2}$$

where $r_{\rm p}$ and $r_{\rm s}$ are the Fresnel reflection coefficients for p- and s-polarized light, respectively. In order to investigate complex samples, ellipsometric measurements should be carried out over a range of wavelengths or incident angles.

Significant developments have been achieved in the field of ellipsometry in the last two decades. Different ellipsometric structures have been proposed theoretically and experimentally.[6−13] The main difference between those structures is the speed ratio with which the optical elements rotate. The most common designs include the rotating analyzer ellipsometer (RAE)[6] and the rotating polarizer and analyzer ellipsometer (RPAE).[7−14] The RAE contains a fixed polarizer and a rotating analyzer with angular speed ω. The RPAE has been proposed in many forms. The most common one is the RPAE with a speed ratio of 1:2.[7,10−12] The RPAE in which the polarizer and the analyzer rotate with a speed ratio of 1:1[8,9] and that with a speed ratio of 1:−1[4] have also been proposed.

In this work, a general ellipsometric configuration is presented using a phase retarder, and the polarizer and the analyzer rotate with 1:N speed ratio. Different special cases are investigated and compared. Two values of the fast axis offset angle of the retarder are considered for each ellipsometric configuration. As a test of the feasibility of these configurations, the optical parameters of c-Si are calculated. The effect of the noise on the results extracted from each ellipsometric configuration and the uncertainties in the ellipsometric parameters as functions of the uncertainties of the Fourier coefficients are studied.

2. Theory of the Mueller formalism

The theory of ellipsometry is usually formulated in terms of the Jones vector or the Mueller matrix. The Jones vector formalism is usually adopted for describing polarized light. In order to describe unpolarized or partially polarized light, the Stokes parameters are usually used. In the actual ellipsometry measurement, the Stokes parameters can be measured. In the

†Corresponding author. E-mail: staya@iugaza.edu.ps

© 2012 Chinese Physical Society and IOP Publishing Ltd

Stokes vector representation, optical elements are described by the Mueller matrix. The Stokes vector consists of four elements, S_0, S_1, S_2, and S_3.

The ellipsometric configurations under consideration consist of a light source, a fixed linear polarizer, a rotating linear polarizer with angular speed ω, a fixed phase retarder, a sample, an analyzer rotating with angular speed ω, and a detector. The phase retarder generates a phase difference between p- and s- light components given by

$$\delta = \frac{2\,\pi\,d}{\lambda}(n_{\rm e} - n_{\rm o}), \tag{3}$$

where d is the thickness of the phase retarder, and $n_{\rm e}$ and $n_{\rm o}$ are the extraordinary and the ordinary refractive indices at wavelength λ.

As the incident light travels through these optical elements, the state of polarization changes. The effect of each element is described by a matrix. The Mueller matrices associated with the optical elements employed in the proposed ellipsometric structure are given as follows.[15] The matrix of rotation with an angle ψ is

$$\boldsymbol{R}(\alpha) = \begin{bmatrix} 1 & 0 & 0 & 0 \\ 0 & \cos(2\psi) & \sin(2\psi) & 0 \\ 0 & -\sin(2\psi) & \cos(2\psi) & 0 \\ 0 & 0 & 0 & 1 \end{bmatrix}. \tag{4}$$

The matrix of an ideal fixed polarizer or analyzer is

$$\boldsymbol{P} = \boldsymbol{A} = \frac{1}{2}\begin{bmatrix} 1 & 1 & 0 & 0 \\ 1 & 1 & 0 & 0 \\ 0 & 0 & 0 & 0 \\ 0 & 0 & 0 & 0 \end{bmatrix}. \tag{5}$$

The matrix of an ideal fixed phase retarder is

$$\boldsymbol{C} = \begin{bmatrix} 1 & 0 & 0 & 0 \\ 0 & 1 & 0 & 0 \\ 0 & 0 & \cos(\delta) & \sin(\delta) \\ 0 & 0 & -\sin(\delta) & \cos(\delta) \end{bmatrix}. \tag{6}$$

The matrix of an ideal sample is

$$\boldsymbol{L} = \begin{bmatrix} 1 & -\cos(2\psi) & 0 & 0 \\ -\cos(2\psi) & 1 & 0 & 0 \\ 0 & 0 & \sin(2\psi)\cos(\Delta) & \sin(2\psi)\sin(\Delta) \\ 0 & 0 & -\sin(2\psi)\sin(\Delta) & \sin(2\psi)\cos(\Delta) \end{bmatrix}. \tag{7}$$

In the ellipsometric configurations under study, the phase retarder is assumed to be fixed with its fast axis having an angle $\beta_{\rm c}$ with the p polarization. We will consider two different orientations of the fixed phase retarder, namely $\beta_{\rm c} = 0^\circ$ and $\beta_{\rm c} = 45^\circ$. For each orientation, we study many ellipsometric configurations by assuming different speed ratios for the rotating elements. The azimuth angle of the rotating polarizer is assumed to be $\beta_{\rm P} = \omega\,t + \tau$ and that of the rotating analyzer is assumed to have the form $\beta_{\rm A} = N\omega\,t + \alpha$, where N is an integer, τ and α are the initial azimuth angles of the polarizer and the analyzer, respectively. While the azimuth angle of the fixed polarizer is assumed to be θ.

The Stokes vector of the detected light of the proposed structure is given by

$$\begin{aligned}\boldsymbol{S} = {} & \boldsymbol{R}(-\beta_{\rm A})\boldsymbol{A}\boldsymbol{R}(\beta_{\rm A})\boldsymbol{L}\boldsymbol{R}(-\beta_{\rm c})\boldsymbol{C}\boldsymbol{R}(\beta_{\rm c}) \\ & \times \boldsymbol{R}(-\beta_{\rm P})\boldsymbol{P}\boldsymbol{R}(\beta_{\rm P})\boldsymbol{R}(-\theta)\boldsymbol{P}\boldsymbol{R}(\theta)\boldsymbol{S}_i, \end{aligned} \tag{8}$$

where $\boldsymbol{S}_i = [1,\,0,\,0,\,0]^{\rm T}$, and $\boldsymbol{S}$ is a four-element column vector containing Stokes parameters S_0, S_1, S_2, and S_3.

3. RPAE with speed ratio 1:N and fixed phase retarder at $\beta_{\rm c} = 0$

After performing the product of matrices given by Eq. (8) and assuming that $\beta_{\rm P} = \omega\,t$ and $\beta_{\rm A} = N\omega\,t$ ($\theta = 0$, $\alpha = 0$, and $\tau = 0$), by rearranging the result, we obtain Stokes-vector elements S_0, S_1, S_2, and S_3. The intensity of the light received by the detector is given by S_0 and is found to be

$$\begin{aligned} I = {} & S_0 \\ = {} & \left[1 - \frac{1}{2}\cos(2\psi)\right] + [1 - \cos(2\psi)]\cos(2\omega t) \\ & - \frac{1}{2}\cos(2\psi)\cos(4\omega t) \\ & + \left[\frac{1}{2} - \cos(2\psi)\right]\cos(2N\omega t) \end{aligned}$$

$$
\begin{aligned}
&+\frac{1}{2}[1-\cos(2\psi)-\sin(2\psi)\cos(\Delta-\delta)]\\
&\times\ \cos 2(N+1)\omega t\\
&+\frac{1}{2}[1-\cos(2\psi)+\sin(2\psi)\cos(\Delta-\delta)]\\
&\times\ \cos 2(N-1)\omega t\\
&+\frac{1}{4}[1-\sin(2\psi)\cos(\Delta-\delta)]\cos 2(N+2)\omega t\\
&+\frac{1}{4}[1+\sin(2\psi)\cos(\Delta-\delta)]\\
&\times\ \cos 2(N-2)\omega t. \qquad (9)
\end{aligned}
$$

The Fourier transform of the detected intensity generates a DC term and $N+2$ AC terms, which may be written as

$$I(t)=a_0+\sum_{n=1}^{N+2}a_n\cos(2n\omega\, t). \qquad (10)$$

Special cases can be obtained by letting $N=1, 2, \ldots$ In the following subsections, we present three special cases in which $N=1$, 2, and 3 respectively. For each ellipsometric configuration, we find the Fourier coefficients, the ellipsometric parameters ψ and Δ in terms of these coefficients, and the uncertainty in the ellipsometric parameters as a function of the uncertainties in the Fourier coefficients.

3.1. RPAE with speed ratio 1:1

The first case we consider here is an RPAE with a speed ratio 1:1. Setting $N=1$ in Eq. (9) and comparing it with Eq. (10), we obtain coefficients a_0, a_1, a_2, and a_3

$$a_0=\frac{3}{2}-\cos(2\psi)+\frac{1}{2}\sin(2\psi)\cos(\Delta-\delta), \qquad (11)$$

$$a_1=\frac{7}{4}-2\cos(2\psi)+\frac{1}{4}\sin(2\psi)\cos(\Delta-\delta), \qquad (12)$$

$$a_2=\frac{1}{2}-\cos(2\psi)-\frac{1}{2}\sin(2\psi)\cos(\Delta-\delta), \qquad (13)$$

$$a_3=\frac{1}{4}[1-\sin(2\psi)\cos(\Delta-\delta)]. \qquad (14)$$

Solving the last three equations for ψ and $\Delta-\delta$ in terms of AC terms a_1, a_2 and a_3, we obtain

$$\sin(\psi)=\sqrt{\frac{a_1+a_3}{2}}, \qquad (15)$$

$$\cos(\psi)=\sqrt{\frac{a_1-4a_2+9a_3}{2}}, \qquad (16)$$

$$\tan(\psi)=\sqrt{\frac{a_1+a_3}{a_1-4a_2+9a_3}}, \qquad (17)$$

$$\cos(\Delta-\delta)=\frac{a_1-2a_2-3a_3}{2\sin(\psi)\cos(\psi)}. \qquad (18)$$

It is important to study the fluctuations of ψ and Δ around their ideal values. Since the sample parameters, layer thicknesses, and the index of refraction are calculated from ψ and Δ, these fluctuations lead to the uncertainties of the sample parameters. The uncertainties $\delta\psi$ and $\delta\Delta$ in ψ and Δ as functions the uncertainties of the Fourier coefficients are obtained by differentiating Eqs. (17) and (18) with respect to a_j ($j=1$, 2, 3) respectively while keeping the other coefficients as constants, we obtain

$$\frac{\delta\psi}{\delta a_1}=\frac{a_2-2a_3}{\sqrt{a_1+a_3}\sqrt{a_1-4a_2+9a_3}(-a_1+2a_2-5a_3)}, \qquad (19)$$

$$\frac{\delta\psi}{\delta a_2}=\frac{-(a_1+a_3)}{\sqrt{a_1+a_3}\sqrt{a_1-4a_2+9a_3}(-a_1+2a_2-5a_3)}, \qquad (20)$$

$$\frac{\delta\psi}{\delta a_3}=\frac{2a_1+a_2}{\sqrt{a_1+a_3}\sqrt{a_1-4a_2+9a_3}(-a_1+2a_2-5a_3)}, \qquad (21)$$

$$\frac{\delta\Delta}{\delta a_1}=\frac{4a_1a_3+12(a_3)^2-2(a_2)^2}{(a_1+a_3)\ (-a_1+4a_2-9a_3)(4a_1a_3-4a_3a_2-(a_2)^2)}, \qquad (22)$$

$$\frac{\delta\Delta}{\delta a_2}=\frac{2a_2-12a_3}{(-a_1+4a_2-9a_3)(4a_1a_3-4a_3a_2-(a_2)^2)}, \qquad (23)$$

$$\frac{\delta\Delta}{\delta a_3}=\frac{-4(a_1)^2+12a_1a_2-12a_1a_3+12a_3a_2-2(a_2)^2}{(a_1+a_3)\ (-a_1+4a_2-9a_3)(4a_1a_3-4a_3a_2-(a_2)^2)}. \qquad (24)$$

3.2. RPAE with speed ratio 1:2

Another ellipsometric configuration can be obtained by letting $N=2$ in Eq. (9). In this case, we obtain the DC term and four AC terms, which may be written as

$$a_0=\frac{5}{4}-\frac{1}{2}\cos(2\psi)+\frac{1}{4}\sin(2\psi)\cos(\Delta-\delta), \qquad (25)$$

$$a_1=\frac{3}{2}-\frac{3}{2}\cos(2\psi)+\frac{1}{2}\sin(2\psi)\cos(\Delta-\delta), \qquad (26)$$

$$a_2 = \frac{1}{2} - \frac{3}{2}\cos(2\psi), \tag{27}$$

$$a_3 = \frac{1}{2} - \frac{1}{2}\cos(2\psi) - \frac{1}{2}\sin(2\psi)\cos(\Delta - \delta), \tag{28}$$

$$a_4 = \frac{1}{4} - \frac{1}{4}\sin(2\psi)\cos(\Delta - \delta). \tag{29}$$

We may evaluate ψ and $\Delta - \delta$ in terms of any coefficient set comprising three Fourier terms. Consequently, excluding the DC term, we have three sets: (a_1, a_2, a_3), (a_1, a_3, a_4), and (a_2, a_3, a_4). The three sets will be studied below.

Case I For set (a_1, a_2, a_3),

$$\sin(\psi) = \sqrt{\frac{a_1 + a_3}{4}}, \tag{30}$$

$$\cos(\psi) = \sqrt{\frac{2a_1 - 2a_2 + a_3}{2}}, \tag{31}$$

$$\tan(\psi) = \sqrt{\frac{a_1 + a_3}{4a_1 - 4a_2 + 2a_3}}, \tag{32}$$

$$\cos(\Delta - \delta) = \frac{a_1 - 3a_3}{4\sin(\psi)\cos(\psi)}. \tag{33}$$

Case II For set (a_1, a_2, a_4),

$$\sin(\psi) = \sqrt{\frac{2a_1 + a_2 + 4a_4}{9}}, \tag{34}$$

$$\cos(\psi) = \sqrt{\frac{4a_1 - 7a_2 + 8a_4}{9}}, \tag{35}$$

$$\tan(\psi) = \sqrt{\frac{2a_1 + a_2 + 4a_4}{4a_1 - 7a_2 + 8a_4}}, \tag{36}$$

$$\cos(\Delta - \delta) = \frac{a_1 - a_2 - 4a_4}{3\sin(\psi)\cos(\psi)}. \tag{37}$$

Case III For set (a_2, a_3, a_4),

$$\sin(\psi) = \sqrt{a_2 - 2a_3 + 4a_4}, \tag{38}$$

$$\cos(\psi) = \sqrt{a_2 - 4a_3 + 8a_4}, \tag{39}$$

$$\tan(\psi) = \sqrt{\frac{a_2 - 2a_3 + 4a_4}{a_2 - 4a_3 + 8a_4}}, \tag{40}$$

$$\cos(\Delta - \delta) = \frac{a_2 - 3a_3 + 4a_4}{\sin(\psi)\cos(\psi)}. \tag{41}$$

The uncertainties $\delta\psi$ and $\delta\Delta$ are calculated for the first set only, and they can be done for the other sets in a similar manner. Differentiating Eqs. (32) and (33) with respect to a_j ($j = 1, 2, 3$) while keeping the other coefficients as constants gives

$$\frac{\delta\Delta}{\delta a_1} = -\frac{1}{Q_1Q_2Q_3} \times \left(1 - \frac{a_1 - 3a_3}{2Q_1^2} - \frac{a_1 - 3a_3}{Q_2^2}\right), \tag{42}$$

$$\frac{\delta\Delta}{\delta a_2} = \frac{-2(a_1 - 3a_3)}{Q_1Q_2^3Q_3}, \tag{43}$$

$$\frac{\delta\Delta}{\delta a_3} = -\frac{1}{Q_1Q_2Q_3} \times \left(-3 - \frac{a_1 - 3a_3}{2Q_1^2} - \frac{a_1 - 3a_3}{Q_2^2}\right), \tag{44}$$

$$\frac{\delta\psi}{\delta a_1} = \frac{Q_2^2 - 2Q_1^2}{2Q_1Q_2(Q_1^2 + Q_2^2)}, \tag{45}$$

$$\frac{\delta\psi}{\delta a_2} = \frac{2Q_1}{Q_2(Q_1^2 + Q_2^2)}, \tag{46}$$

$$\frac{\delta\psi}{\delta a_3} = \frac{Q_2^2 - 2Q_1^2}{2Q_1Q_2(Q_1^2 + Q_2^2)}, \tag{47}$$

where

$$Q_1 = \sqrt{a_1 + a_3}, \tag{48}$$

$$Q_2 = \sqrt{2a_1 - 4a_2 + 2a_3}, \tag{49}$$

$$Q_3 = \sqrt{1 - \frac{(a_1 - 3a_3)^2}{(a_1 + a_3)(2a_1 - 4a_2 + 2a_3)}}. \tag{50}$$

3.3. RPAE with speed ratio 1:3

In the third case, we assume an ellipsometric configuration in which the polarizer and the analyzer rotate at speed ratio 1:3. Setting $N = 3$ in Eqs. (9) and (10) to find the intensity and the Fourier coefficients of this configuration, we obtain

$$a_0 = 1 - \frac{1}{2}\cos(2\psi), \tag{51}$$

$$a_1 = \frac{5}{4} - \cos(2\psi) + \frac{1}{4}\sin(2\psi)\cos(\Delta - \delta), \tag{52}$$

$$a_2 = \frac{1}{2} - \cos(2\psi) + \frac{1}{2}\sin(2\psi)\cos(\Delta - \delta), \tag{53}$$

$$a_3 = \frac{1}{2} - \cos(2\psi), \tag{54}$$

$$a_4 = \frac{1}{2} - \frac{1}{2}\cos(2\psi) - \frac{1}{2}\sin(2\psi)\cos(\Delta - \delta), \tag{55}$$

$$a_5 = \frac{1}{4} - \frac{1}{4}\sin(2\psi)\cos(\Delta - \delta). \tag{56}$$

In analogy to the 1:2 configuration, we have many sets from which the ellipsometric parameters can be obtained. When the speed ratio is 1:3, six sets can be taken without considering the DC term. Some of these cases are listed below.

Case I For set (a_1, a_2, a_3),

$$\sin(\psi) = \sqrt{\frac{2a_1 - a_2 + 2a_3}{6}}, \tag{57}$$

$$\cos(\psi) = \sqrt{\frac{2a_1 - a_2 - 2a_3}{2}}, \tag{58}$$

$$\tan(\psi) = \sqrt{\frac{2a_1 - a_2 + 2a_3}{3(2a_1 - a_2 - 2a_3)}}, \tag{59}$$

$$\cos(\Delta - \delta) = \frac{-a_3 + a_2}{\sin(\psi)\cos(\psi)}. \tag{60}$$

Case II For set (a_1, a_2, a_4),

$$\sin(\psi) = \sqrt{\frac{2a_1 + a_2 + 2a_4}{4}}, \tag{61}$$

$$\cos(\psi) = \sqrt{\frac{10a_1 - 11a_2 - 6a_4}{4}}, \tag{62}$$

$$\tan(\psi) = \sqrt{\frac{2a_1 + a_2 + 2a_4}{10a_1 - 11a_2 - 6a_4}}, \tag{63}$$

$$\cos(\Delta - \delta) = \frac{2a_1 + a_2 - 6a_4}{4\sin(\psi)\cos(\psi)}. \tag{64}$$

Case III For set (a_1, a_2, a_5),

$$\sin(\psi) = \sqrt{2a_2 + 4a_5}, \tag{65}$$

$$\cos(\psi) = \sqrt{8a_1 - 10a_2 - 12a_5}, \tag{66}$$

$$\tan(\psi) = \sqrt{\frac{2a_2 + 4a_5}{8a_1 - 10a_2 - 12a_5}}, \tag{67}$$

$$\cos(\Delta - \delta) = \frac{4a_1 - 4a_2 - 12a_5}{\sin(\psi)\cos(\psi)}. \tag{68}$$

Case IV For set (a_2, a_3, a_4),

$$\sin(\psi) = \sqrt{2a_2 - 2a_3 + 2a_4}, \tag{69}$$

$$\cos(\psi) = \sqrt{6a_2 - 10a_3 + 6a_4}, \tag{70}$$

$$\tan(\psi) = \sqrt{\frac{2a_2 - 2a_3 + 2a_4}{6a_2 - 10a_3 + 6a_4}}, \tag{71}$$

$$\cos(\Delta - \delta) = \frac{2a_2 - 2a_3}{\sin(\psi)\cos(\psi)}. \tag{72}$$

Differentiating Eqs. (59) and (60) with respect to a_j ($j = 1, 2, 3$) while keeping the other coefficients as constants gives the uncertainties as follows:

$$\frac{\delta\Delta}{\delta a_1} = \frac{A_4}{A_2^3 A_3^3 A_1}\left(\frac{2}{3}A_3^2 + 2A_2^2\right), \tag{73}$$

$$\frac{\delta\Delta}{\delta a_2} = \frac{-1}{A_1 A_2 A_3}\left[4 + \frac{A_4\left(A_3^2 + 3A_2^2\right)}{3A_2^2 A_3^2}\right], \tag{74}$$

$$\frac{\delta\Delta}{\delta a_3} = \frac{-1}{A_1 A_2 A_3}\left[-4 - \frac{2A_4\left(A_3^2 - 3A_2^2\right)}{3A_2^2 A_3^2}\right], \tag{75}$$

$$\frac{\delta\psi}{\delta a_1} = \left[\frac{2A_3^2 - 6A_2^2}{3A_2 A_3\left(A_3^2 + A_2^2\right)}\right], \tag{76}$$

$$\frac{\delta\psi}{\delta a_2} = \left[\frac{-A_3^2 + 3A_2^2}{3A_2 A_3\left(A_3^2 + A_2^2\right)}\right], \tag{77}$$

$$\frac{\delta\psi}{\delta a_3} = \left[\frac{2A_3^2 + 6A_2^2}{3A_2 A_3\left(A_3^2 + A_2^2\right)}\right], \tag{78}$$

where

$$A_1 = \sqrt{1 - \frac{A_4^2}{A_2^2 A_3^2}}, \tag{79}$$

$$A_2 = \sqrt{\frac{4a_1 - 2a_2 + 4a_3}{3}}, \tag{80}$$

$$A_3 = \sqrt{4a_1 - 2a_2 - 4a_3}, \tag{81}$$

$$A_4 = 4a_2 - 4a_3. \tag{82}$$

4. RPAE with speed ratio 1:N and fixed phase retarder at $\beta_c = 45°$

The orientation of the phase retarder is a key parameter affecting the results extracted from the proposed ellipsometric configurations. To introduce this point in our study, we assume another orientation for the phase retarder $\beta_c = 45°$. The product of matrices given by Eq. (8) is performed again with $\beta_c = 45°$. Stokes vector elements are then obtained. As mentioned before, the detected intensity is given by S_0

$$\begin{aligned} I &= S_0 \\ &= \left[1 - \frac{1}{2}\cos(2\psi)\cos(\delta)\right] \\ &\quad + [1 - \cos(2\psi)\cos(\delta)]\cos(2\omega t) \\ &\quad - \frac{1}{2}\cos(2\psi)\cos(\delta)\cos(4\omega t) \\ &\quad + \left[\frac{\cos(\delta)}{2} - \cos(2\psi)\right]\cos(2N\omega t) \\ &\quad + \frac{1}{2}[\cos(\delta) - \cos(2\psi) - \sin(2\psi)\cos(\Delta)] \\ &\quad \times \cos 2(N+1)\omega t \\ &\quad + \frac{1}{2}[\cos(\delta) - \cos(2\psi) + \sin(2\psi)\cos(\Delta)] \\ &\quad \times \cos 2(N-1)\omega t \\ &\quad + \frac{1}{4}[\cos(\delta) - \sin(2\psi)\cos(\Delta)]\cos 2(N+2)\omega t \\ &\quad + \frac{1}{4}[\cos(\delta) + \sin(2\psi)\cos(\Delta)]\cos 2(N-2)\omega t \\ &\quad + \frac{1}{2}[\sin(2\psi)\sin(\Delta)\sin(\delta)]\sin(2N\omega\, t) \\ &\quad + \frac{1}{2}[\sin(2\psi)\sin(\Delta)\sin(\delta)]\sin 2(N+1)\omega\, t \\ &\quad + \frac{1}{2}[\sin(2\psi)\sin(\Delta)\sin(\delta)]\sin 2(N-1)\omega\, t \\ &\quad + \frac{1}{4}[\sin(2\psi)\sin(\Delta)\sin(\delta)]\sin 2(N+2)\omega\, t \\ &\quad + \frac{1}{4}[\sin(2\psi)\sin(\Delta)\sin(\delta)]\sin 2(N-2)\omega\, t. \end{aligned} \tag{83}$$

The Fourier transform of the detected intensity generates a DC term, $(N + 2)$ cosine AC terms, and $(N + 2)$ sine AC terms, which may be written as

$$\begin{aligned} I(t) &= a_0 + \sum_{n=1}^{N+2} a_n \cos(2n\omega\, t) \\ &\quad + \sum_{n=1}^{N+2} b_n \sin(2n\omega\, t). \end{aligned} \tag{84}$$

The following subsections show three special cases in which $N = 1$, 2, and 3 respectively.

4.1. RPAE with speed ratio 1:1

We first consider the case with $N = 1$ in Eqs. (83) and (84). The comparison between the results gives coefficients a_1, a_2, a_3, b_1, b_2, and b_3 as

$$a_1 = 1 - \cos(2\psi)\cos(\delta) - \cos(2\psi) + \frac{6}{8}\cos(\delta) + \frac{1}{4}\sin(2\psi)\cos(\Delta), \quad (85)$$

$$a_2 = -\frac{1}{2}\cos(2\psi)\cos(\delta) - \frac{1}{2}\cos(2\psi) + \frac{1}{2}\cos(\delta) - \frac{1}{2}\sin(2\psi)\cos(\Delta), \quad (86)$$

$$a_3 = \frac{1}{4}\cos(\delta) - \frac{1}{4}\sin(2\psi)\cos(\Delta), \quad (87)$$

$$b_1 = \frac{1}{4}\sin(2\psi)\sin(\Delta)\sin(\delta), \quad (88)$$

$$b_2 = \frac{1}{2}\sin(2\psi)\sin(\Delta)\sin(\delta), \quad (89)$$

$$b_3 = \frac{1}{4}\sin(2\psi)\sin(\Delta)\sin(\delta). \quad (90)$$

As mentioned above, only three coefficients are needed to calculate the ellipsometric parameters. If we consider again a_1, a_2, and a_3 and solve Eqs. (85), (86), and (87), ψ and Δ are given by

$$\tan(\psi) = \sqrt{\frac{a_1 + a_3}{a_1 - 4a_2 + 9a_3}}, \quad (91)$$

$$\cos(\Delta) = \frac{2\,(a_1 - 2a_2 + a_3 - 4a_3/\cos(\delta))\,\cos(\delta)}{\sqrt{2a_1 + 2a_3}\sqrt{2a_1 - 8a_2 + 18a_3}}. \quad (92)$$

The comparison of Eqs. (91) and (92) with Eqs. (17) and (18) shows the independence of ψ and the dependence of Δ on β_c. As a result, the uncertainty $\delta\psi$ is still given by Eqs. (19), (20), and (21) whereas $\delta\Delta$ is given by

$$\frac{\delta\Delta}{\delta a_1} = -\frac{2T - RT/(2a_1 + 2a_3) - RT/(2a_1 - 8a_2 + 18a_3)}{\sqrt{1 - T^2R^2}}, \quad (93)$$

$$\frac{\delta\Delta}{\delta a_2} = \frac{4T - 4RT/(2a_1 - 8a_2 + 18a_3)}{\sqrt{1 - T^2R^2}}, \quad (94)$$

$$\frac{\delta\Delta}{\delta a_3} = -\frac{(2 - 8/\cos(\delta))\,T - RT/(2a_1 + 2a_3) - 9RT/(2a_1 - 8a_2 + 18a_3)}{\sqrt{1 - T^2R^2}}, \quad (95)$$

where

$$T = \frac{\cos(\delta)}{\sqrt{2a_1 + 2a_3}\sqrt{2a_1 - 8a_2 + 18a_3}}, \quad (96)$$

$$R = 2a_1 - 4a_2 + 2a_3 - \frac{8\,a_3}{\cos(\delta)}. \quad (97)$$

4.2. RPAE with speed ratio 1:2

Letting $N = 2$ in Eq. (83) and comparing with Eq. (84), we obtain, in addition to the DC term, eight AC terms given by

$$a_1 = 1 - \cos(2\psi)\cos(\delta) - \frac{1}{2}\cos(2\psi) + \frac{1}{2}\cos(\delta) + \frac{1}{2}\sin(2\psi)\cos(\Delta), \quad (98)$$

$$a_2 = -\frac{1}{2}\cos(2\psi)\cos(\delta) - \cos(2\psi) + \frac{1}{2}\cos(\delta), \quad (99)$$

$$a_3 = -\frac{1}{2}\cos(2\psi) - \frac{1}{2}\cos(2\delta) - \frac{1}{2}\sin(2\psi)\cos(\Delta), \quad (100)$$

$$a_4 = \frac{1}{4}\cos(\delta) - \frac{1}{4}\sin(2\psi)\cos(\Delta), \quad (101)$$

$$b_1 = \frac{1}{2}\sin(2\psi)\sin(\Delta)\sin(\delta), \quad (102)$$

$$b_2 = \frac{1}{2}\sin(2\psi)\sin(\Delta)\sin(\delta), \quad (103)$$

$$b_3 = \frac{1}{2}\sin(2\psi)\sin(\Delta)\sin(\delta), \quad (104)$$

$$b_4 = \frac{1}{4}\sin(2\psi)\sin(\Delta)\sin(\delta). \quad (105)$$

A large number of three-term sets can be obtained to extract the ellipsometric parameters. We restrict ourselves to the first set including (a_1, a_2, a_3). Solving Eqs. (98), (99), and (100) for ψ and Δ, we obtain

$$\tan(\psi) = \sqrt{\frac{a_1 + a_3}{(a_1 - 2a_2 + a_3)\,(1 + \cos(\delta))}}, \quad (106)$$

$$\cos(\Delta) = \frac{\cos(\delta)a_1/2 + (1 - \cos(\delta))\,a_2 - (4 - \cos(\delta))\,a_3/2}{\sqrt{(a_1 + a_3)/(1 + \cos(\delta))}\sqrt{a_1 - 2a_2 + a_3}}. \quad (107)$$

Differentiating the last two equations to find the uncertainty in the ellipsometric parameters due to the uncertainties in the Fourier coefficients, we obtain

$$\frac{\delta\psi}{\delta a_1} = -2B_1B_2B_3a_2, \quad (108)$$

$$\frac{\delta\psi}{\delta a_2} = 2B_1B_2B_3\,(a_1 + a_3)\,, \quad (109)$$

$$\frac{\delta\psi}{\delta a_3} = -2B_1B_2B_3a_2. \quad (110)$$

with

$$B_1 = \frac{1}{1+\tan^2(\psi)}, \tag{111}$$

$$B_2 = \frac{1}{2\tan(\psi)}, \tag{112}$$

$$B_3 = \frac{1}{(a_1-2a_2+a_3)^2(1+\cos(\delta))}; \tag{113}$$

and

$$\frac{\delta\Delta}{\delta a_1} = \frac{1}{4\sin(\Delta)\sin(\psi)\cos(\psi)} \times \left[-\cos(\delta)+\cos(\Delta) \times \left(\tan(\psi)+\frac{\cot(\psi)}{1+\cos(\delta)}\right)\right], \tag{114}$$

$$\frac{\delta\Delta}{\delta a_2} = \frac{1}{2\sin(\Delta)\sin(\psi)\cos(\psi)} \times \left[-1+\cos(\delta)-\cos(\Delta)\tan(\psi)\right], \tag{115}$$

$$\frac{\delta\Delta}{\delta a_3} = \frac{1}{4\sin(\Delta)\sin(\psi)\cos(\psi)} \times \left[4-\cos(\delta)+\cos(\Delta) \times \left(\tan(\psi)+\frac{\cot(\psi)}{1+\cos(\delta)}\right)\right]. \tag{116}$$

4.3. RPAE with speed ratio 1:3

The last case to be considered has $N = 3$. Following the same methodology as above, the AC Fourier coefficients are found to be

$$a_1 = 1-\cos(2\psi)\cos(\delta)+\frac{1}{4}\cos(\delta) + \frac{1}{4}\sin(2\psi)\cos(\Delta), \tag{117}$$

$$a_2 = -\frac{1}{2}\cos(2\psi)\cos(\delta)-\frac{1}{2}\cos(2\psi)+\frac{1}{2}\cos(\delta) + \frac{1}{2}\sin(2\psi)\cos(\Delta), \tag{118}$$

$$a_3 = -\cos(2\psi)+\frac{1}{2}\cos(2\delta), \tag{119}$$

$$a_4 = -\frac{1}{2}\cos(2\psi)+\frac{1}{2}\cos(\delta) - \frac{1}{2}\sin(2\psi)\cos(\Delta), \tag{120}$$

$$a_5 = \frac{1}{4}\cos(\delta)-\frac{1}{4}\sin(2\psi)\cos(\Delta), \tag{121}$$

$$b_1 = \frac{1}{4}\sin(2\psi)\sin(\Delta)\sin(\delta), \tag{122}$$

$$b_2 = \frac{1}{2}\sin(2\psi)\sin(\Delta)\sin(\delta), \tag{123}$$

$$b_3 = \frac{1}{2}\sin(2\psi)\sin(\Delta)\sin(\delta), \tag{124}$$

$$b_4 = \frac{1}{2}\sin(2\psi)\sin(\Delta)\sin(\delta), \tag{125}$$

$$b_5 = \frac{1}{4}\sin(2\psi)\sin(\Delta)\sin(\delta). \tag{126}$$

The first set including coefficients (a_1, a_2, a_3) is only assumed. The ψ and Δ are calculated as

$$\sin(\psi) = \sqrt{\frac{(4-2\cos(\delta))\,a_1-(2-\cos(\delta))\,a_2+(5-3\cos(\delta))\,a_3}{D_0}}, \tag{127}$$

$$\cos(\psi) = \sqrt{\frac{(4+2\cos(\delta))\,a_1-(2+\cos(\delta))\,a_2-(3+3\cos(\delta))\,a_3}{D_0}}, \tag{128}$$

$$\tan(\psi) = \sqrt{\frac{(4-2\cos(\delta))\,a_1-(2-\cos(\delta))\,a_2+(5-3\cos(\delta))\,a_3}{(4+2\cos(\delta))\,a_1-(2+\cos(\delta))\,a_2-(3+3\cos(\delta))\,a_3}}, \tag{129}$$

$$\cos(\Delta) = \frac{\left[2\,(a_2-a_3)/(1-\cos(\delta))+\sin^2(\psi)-\cos^2(\psi)\right](1-\cos(\delta))}{2\,\sin(\psi)\,\cos(\psi)}. \tag{130}$$

Finally, we find the uncertainties in the ellipsometric coefficients as

$$\frac{\delta\psi}{\delta a_1} = \frac{1}{2\sin(\psi)\cos(\psi)} \times \left(\frac{4\cos(2\psi)}{D_0}-\frac{2\cos(\delta)}{D_0}\right), \tag{131}$$

$$\frac{\delta\psi}{\delta a_2} = \frac{1}{2\sin(\psi)\cos(\psi)} \times \left(\frac{-2\cos(2\psi)}{D_0}+\frac{\cos(\delta)}{D_0}\right), \tag{132}$$

$$\frac{\delta\psi}{\delta a_3} = \frac{1}{2\sin(\psi)\cos(\psi)}$$

$$\times \left(D_8 \cos(2\psi) + \frac{8\cos^2(\psi)}{D_0} \right), \quad (133)$$

$$\frac{\delta\Delta}{\delta a_1} = \frac{1}{\sin(\Delta) 2\sin(\psi)\cos(\psi)} \times [D_1 + \cos(\Delta)(D_2 \tan(\psi) + D_3 \cot(\psi)], \quad (134)$$

$$\frac{\delta\Delta}{\delta a_2} = \frac{1}{\sin(\Delta) 2\sin(\psi)\cos(\psi)} \times [D_4 + \cos(\Delta)(D_5 \tan(\psi) + D_6 \cot(\psi)], \quad (135)$$

$$\frac{\delta\Delta}{\delta a_3} = \frac{1}{\sin(\Delta) 2\sin(\psi)\cos(\psi)} \times [D_7 + \cos(\Delta)(D_8 \tan(\psi) + D_9 \cot(\psi)], \quad (136)$$

where

$$D_0 = 8 + \cos(\delta) - 3\cos^2(\delta), \quad (137)$$

$$D_1 = \frac{4\cos(\delta) - 4\cos^2(\delta)}{D_0}, \quad (138)$$

$$D_2 = \frac{4 + 2\cos(\delta)}{D_0}, \quad (139)$$

$$D_3 = \frac{4 - 2\cos(\delta)}{D_0}, \quad (140)$$

$$D_4 = \frac{-16 - 4\cos(\delta) + 8\cos^2(\delta)}{D_0}, \quad (141)$$

$$D_5 = \frac{-2 - \cos(\delta)}{D_0}, \quad (142)$$

$$D_6 = \frac{-2 + \cos(\delta)}{D_0}, \quad (143)$$

$$D_7 = \frac{8 + 12\cos(\delta) - 6\cos^2(\delta)}{D_0}, \quad (144)$$

$$D_8 = \frac{-3 - 3\cos(\delta)}{D_0}, \quad (145)$$

$$D_9 = \frac{5 - 3\cos(\delta)}{D_0}. \quad (146)$$

5. Results and discussion

5.1. The noise effect

The applicability of the proposed structure is tested numerically in this section by considering a sample of one interface separating a semi-infinite air layer of refractive index N_0 and a bulk c-Si material of refractive index N_1. We assume an incidence angle of 70°, which is the most common angle used in spectroscopic ellipsometry. The real and the imaginary parts of the refractive index of c-Si are taken from the handbook of optical constants of solids.[16] Phase retarders made of MgF_2 are extensively used in ellipsometric measurements. We consider a zero-order MgF_2 phase retarder centered at 4 eV.

The general approach used to obtain the ellipsometric coefficients is as follows. The Fresnel reflection coefficients are calculated for the one-interface structure assumed. All of the matrices given by Eqs. (4)–(7) are then found. From the product of these matrices, the intensity received by the detector is calculated, which is element S_0 of the matrix. The Fourier transform of the signal is taken to extract the Fourier coefficients. The ellipsometric parameters ψ and Δ are then found in the photon energy range 1.5–6 eV using the Fourier coefficients. These values of the ellipsometric parameters correspond to the clean signal without considering any noise. Such a case with no noise is not realistic. In real situations, random fluctuations in the recorded signal appear due to the noise from many sources. To simulate the realistic case, noise was generated using MathCAD code and was superimposed on the clean signal according to the following equation:

$$I_{\text{noise}} = (\text{rnd}(c) - c/2)I + (\text{rnd}(e) - e/2) + 0.0001 I_{\max}, \quad (147)$$

where MathCAD's rnd(c) function produces the random noise in the range from 0 to c, and the rnd(e) function produces the random noise in the range from 0 to e. Figure 1 shows the noise superimposed on the clean signal.

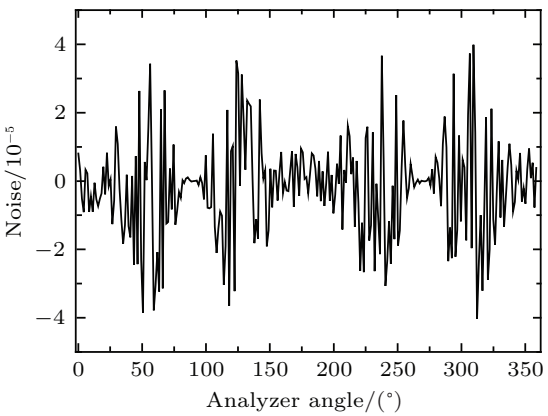


Fig. 1. Noise superimposed on the clean signal.

The noise is added to the pure signal. The Fourier transform of the noisy signal is taken to extract new coefficients a_0–a_n in the presence of the noise.

To calculate the complex refractive index of the sample, we use the well known equation

$$\varepsilon_{\rm r} = \sin^2\theta_0 + \sin^2\theta_0 \tan^2\theta_0 \left(\frac{1-\rho}{1+\rho}\right)^2, \qquad (148)$$

where $\rho = r_{\rm p}/r_{\rm s} = \tan\psi\, {\rm e}^{{\rm i}\Delta}$, $\varepsilon_{\rm r} = \varepsilon_1 + {\rm i}\varepsilon_2$, $\tilde{n} = \sqrt{\varepsilon} = n + {\rm i}k$, $\varepsilon_1 = n^2 - k^2$, and $\varepsilon_2 = 2nk$.

The calculated values of the real (n) and the imaginary (k) parts of the refractive index of c-Si are plotted in Fig. 2 along with the published values.[16] The points in Fig. 2 represent the calculated n and k of c-Si using the noisy signal. These points are calculated using any ellipsometric configuration of the six mentioned above. We have six different ellipsometric configurations. The difference between them is not obvious in this figure. To differentiate between them, we calculate the percent errors in the calculated values of n and k for each ellipsometric configuration.

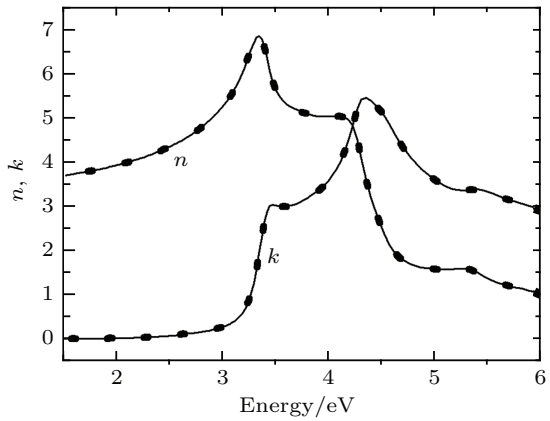


Fig. 2. Real and imaginary parts of the refractive index of c-Si in the photon energy range from 1.5 eV to 6 eV. Lines and points represent accepted and calculated values, respectively.

The percent errors in the calculated values of n for c-Si are shown in Fig. 3 using the set containing (a_1, a_2, a_3). The figure shows the errors arising from calculating n using six different structures which are 1:1, 1:2, and 1:3 with $\beta_{\rm c}$ equaling to either 0° or 45°. The fluctuations shown in the figure are due to the noise imposed on the clean signal as mentioned before. As can be seen from the figure, the percent error in n has small values (of order 10^{-2}) for all ellipsometric configurations with a clear preference of structures having $\beta_{\rm c} = 0°$ over those with $\beta_{\rm c} = 45°$. The percent errors in n at high energies are relatively high (for all ellipsometric configurations) compared to those in the low energy region due to the relatively small values of n at high energies.

Figure 4 shows the percent error in k in the photon energy range from 1.5 eV to 3 eV. The range from 3 eV to 6 eV is not plotted because the error in k almost goes to zero in this region. The percent error in k is much higher than that in n in the low energy region. That is because the imaginary part k is very sensitive to the noise imposed on the signal. Generally, the percent error is considerable for k because it has a small value (0.019) at the wavelength of 632.8 nm. The figure shows clearly a considerable preference of the ellipsometric configurations having $\beta_{\rm c} = 0°$ over those with $\beta_{\rm c} = 45°$. Moreover, for the same $\beta_{\rm c}$, the structure with speed ratio 1:1 has much less percent error compared to the structures having speed ratios 1:2 and 1:3. This result is compatible with the results obtained in Ref. [17].

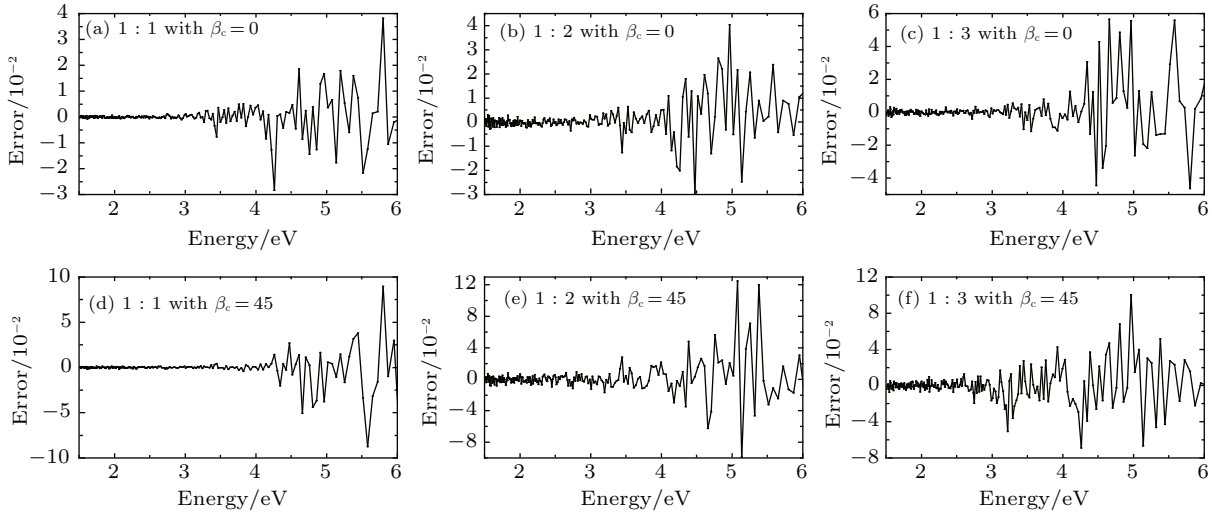


Fig. 3. Percent errors in the real part of the refractive index of c-Si in the photon energy range from 1.5 eV to 6 eV for six different structures ((a)–(f)).

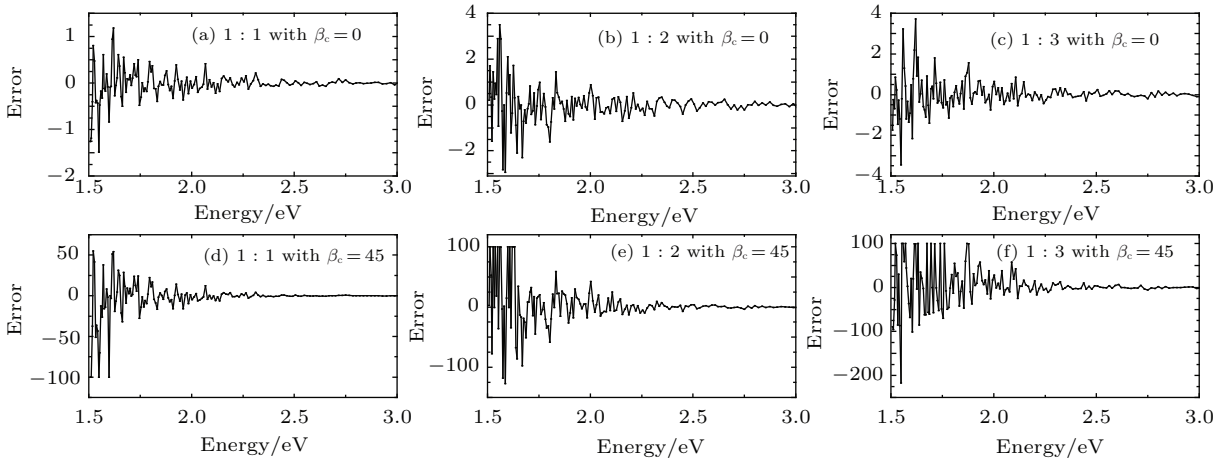


Fig. 4. Percent errors in the imaginary part of the refractive index of c-Si in the photon energy range from 1.5 eV to 3 eV for six different structures ((a)–(f)).

5.2. Uncertainties in ψ and Δ

We now turn our attention to the uncertainties $\delta\psi$ and $\delta\Delta$ in ψ and Δ as functions of the uncertainties of the Fourier coefficients. Figure 5 shows $\delta\psi$ versus the photon energy in the spectral range from 1.5 eV to 6 eV for the six ellipsometric configurations under study. Generally, the sensitivity exhibited by ψ to the uncertainties of the Fourier coefficients is not considerable for all ellipsometric structures. Compared to the sensitivity in the high energy region, a relatively high sensitivity of ψ at low energies is observed in the figure. As can be seen from the figure, the uncertainty of ψ does not depend of β_c. A small dependence of $\delta\psi$ on the speed ratio at which the polarizer and the analyzer rotate can been seen, the 1:3 configuration has the highest sensitivity.

The phase change Δ is more sensitive to the uncertainties in the Fourier coefficients than ψ. Figure 6 shows the uncertainty of Δ with respect to the uncertainties of the Fourier coefficients versus the photon energy for the six ellipsometric configurations under study. Many interesting features can be seen in the figure. First, in analogy to $\delta\psi$, at low energies, where c-Si is essentially transparent, the sensitivity of Δ is high compared to that in the high-energy region. Second, there is a strong dependence of $\delta\Delta$ on β_c. The phase change Δ is more sensitive to the uncertainties in the Fourier coefficients when $\beta_c = 45°$ than that in the case when $\beta_c = 0°$. For $\beta_c = 45°$, the sensitivity of Δ exceeds 400 for some cases, whereas it does not exceed 5 for all configurations when $\beta_c = 0°$. This enhances the conclusion mentioned above that there is a considerable preference of the ellipsometric configurations having $\beta_c = 0°$ over those with $\beta_c = 45°$. Third,

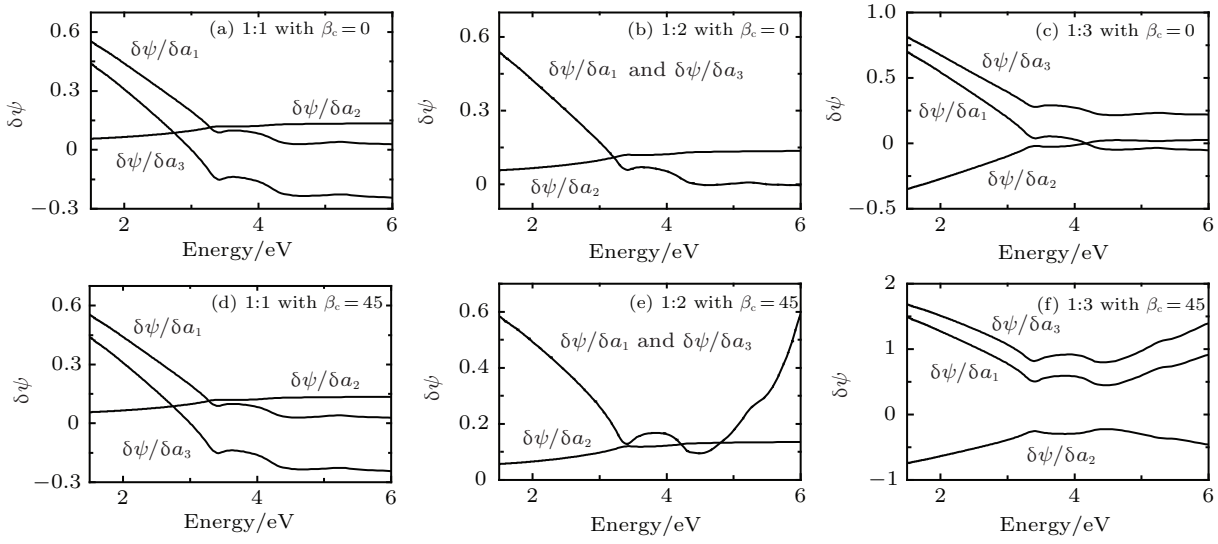


Fig. 5. The variations in ψ for all structures versus the photon energy for six different structrues ((a)–(f)).

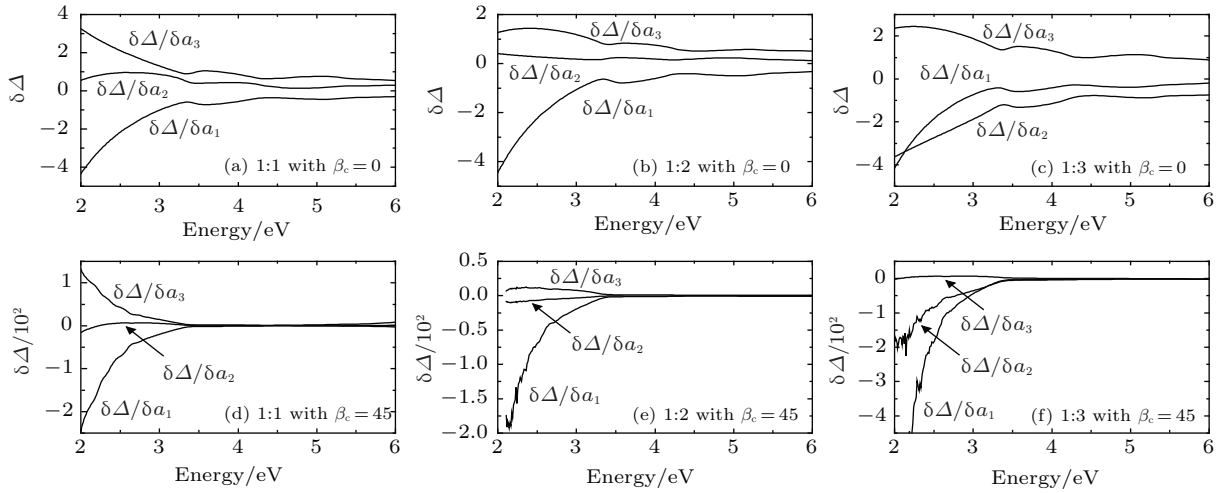


Fig. 6. The variations in Δ for all structures versus the photon energy for six different structrues ((a)–(f)).

the sensitivity of Δ to coefficient a_2 has the lowest values for most cases. Fourth, the maximum sensitivity can be seen in the ellipsometric configuration with speed ratio 1:3 and $\beta_c = 45°$.

5.3. Offset error

In reality, random and systematic errors are the main error sources affecting ellipsometric measurements. The random errors are attributed to random or statistical processes, while the systematic errors result from the experimental setup errors. In ellipsometric measurements, the random errors could be due to the thermally generated noise in the electronic elements. This type of error can be significantly reduced by signal averaging of multiple identical runs and by calculating the mean and the standard deviation. On the other hand, the systematic errors can be reduced by careful calibration of a high quality optical element setup. Some sources of systematic errors are due to the azimuthally misalignment of the optical elements with respect to the plane of incidence, the sample mispositioning, the beam deviation, and the collimation errors.[4] The other sources of systematic error could be the light wavelength and the angle of incidence. Therefore, it is very important to study the systematic

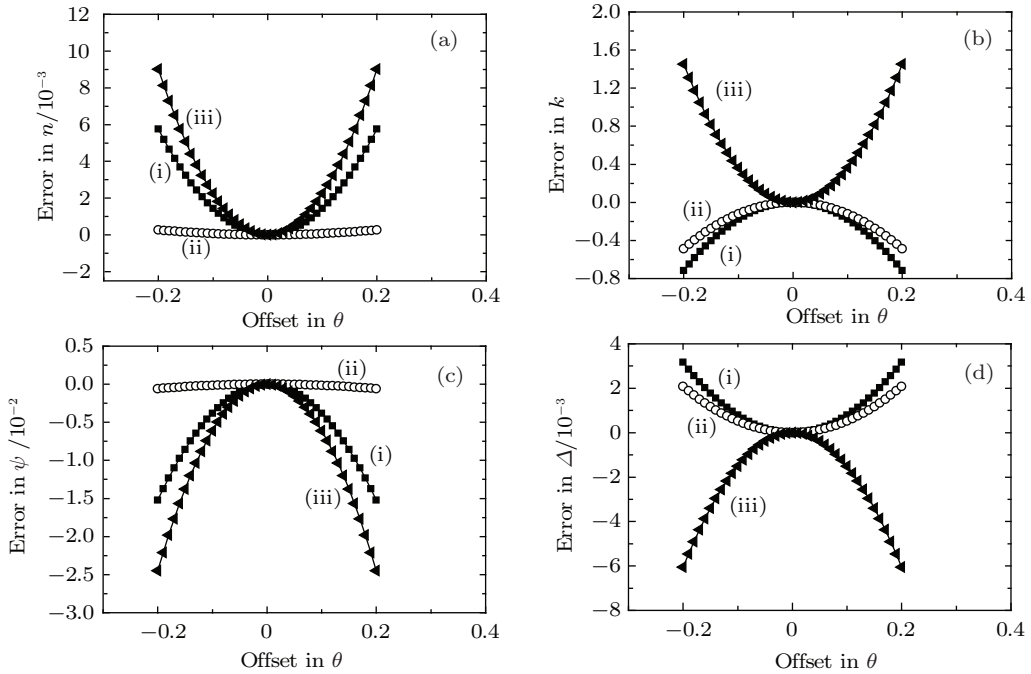


Fig. 7. Percent errors in (a) n, (b) k, (c) ψ, and (d) Δ for c-Si sample at $\lambda = 632.8$ nm each as a function of the error in θ while keeping the two other variables (τ and α) equal to zero, where the speed ratios are (i) 1:1, (ii) 1:2, and (iii) 1:3.

errors in the proposed structure. For the verification process, we will assume a misalignment of the fixed polarizer, the rotating polarizer, and the rotating analyzer. The effect of the misalignment on ψ, Δ, n, and k will be investigated. We will restrict the following calculations to the case with $\beta_c = 0$. Figure 7 shows the percent errors in ψ, Δ, n, and k for the three ellipsometric configurations at $\beta_c = 0$ each as a function of the error of the fixed polarizer azimuth angle θ varied from -0.2° to 0.2° in steps of 0.01° while keeping the other two variables (τ and α) equal to zero. As can be seen from the figure, the impact of these errors on ψ, Δ, and n is not significant for small misalignment in θ. On the other hand, it is relatively considerable for k in the ellipsometric configuration with ratio 1:3. The figure also reveals that the ellipsometric configuration with speed ratio 1:2 shows the lowest impact on the parameters under investigation. On the other hand, the ellipsometric configuration with speed ratio 1:3 shows the highest impact on these parameters.

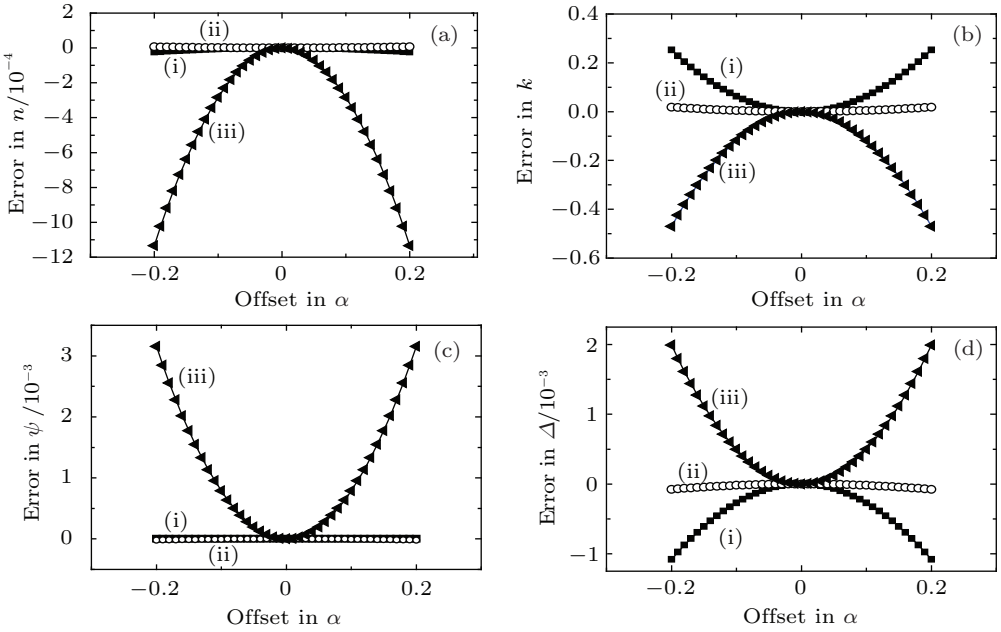


Fig. 8. Percent errors in (a) n, (b) k, (c) ψ, and (d) Δ for c-Si sample at $\lambda = 632.8$ nm each as a function of the error in α while keeping the two other variables (τ and θ) equal to zero, where the speed ratios are (i) 1:1, (ii) 1:2, and (iii) 1:3.

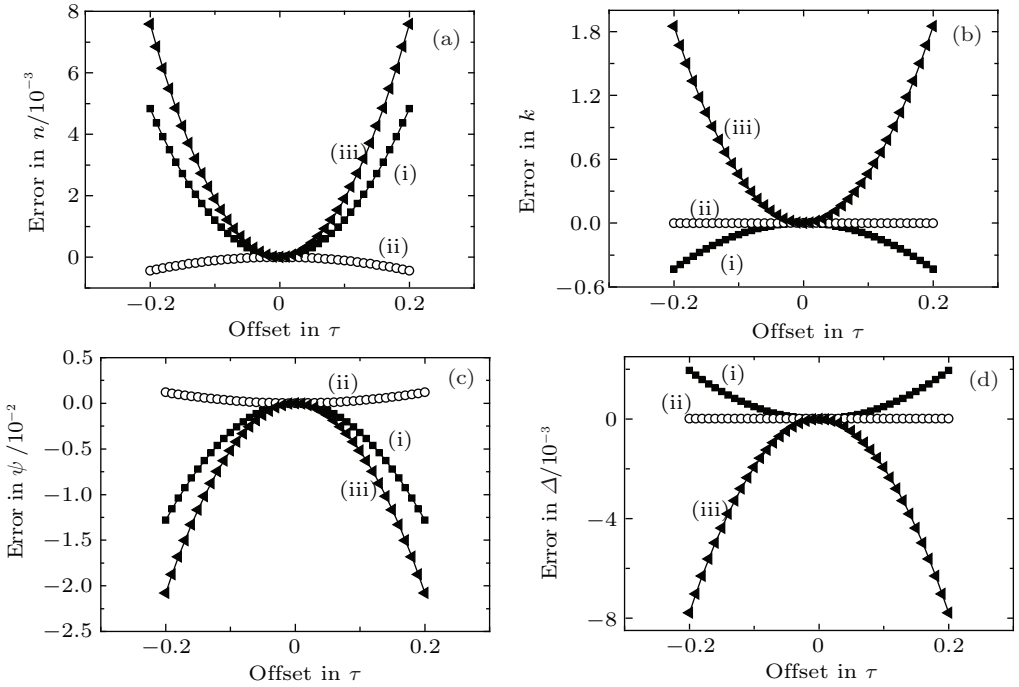


Fig. 9. Percent errors in (a) n, (b) k, (c) ψ, and (d) Δ for c-Si sample at $\lambda = 632.8$ nm each as a function of the error in τ while keeping the two other variables (θ and α) equal to zero, where the speed ratios are (i) 1:1, (ii) 1:2, and (iii) 1:3.

In analogy to Fig. 7, Fig. 8 shows the percent errors in ψ, Δ, n, and k for the three ellipsometric configurations each as a function of the error of the rotating analyzer initial azimuth angle α varied from -0.2° to 0.2° in steps of 0.01° while keeping the other two variables (τ and θ) equal to zero. The figure reveals the same observations that have been seen in Fig. 7. Any misalignment in the rotating analyzer azimuth angle has a neglected impact on ψ, Δ, and n and a relatively considerable impact on k. The structure with speed ratio 1:2 has the minimum percent error in these parameters among all structures, whereas the maximum error is accompanied with the structure having speed ratio 1:3.

The percent errors in ψ, Δ, n, and k for the three ellipsometric configurations each as a function of the error of the rotating polarizer initial azimuth angle τ is plotted in Fig. 9. The same comments that have been extracted from Figs. 7 and 8 can also be applied to Fig. 9.

6. Conclusion

A rotating polarizer–analyzer ellipsometer using a phase retarder is proposed. Based on the speed ratio at which the polarizer and the analyzer rotate, different ellipsometric configurations are presented and compared. Moreover, two different alignments for the retarder are considered for each ellipsometric configuration. All configurations are applied to a bulk c-Si to extract the optical parameters. A comparison between different configurations is carried out considering the effect of the hypothetical noise on the results, the uncertainties in the ellipsometric parameters as functions of the uncertainties of the Fourier coefficients, and the error arising from the misalignment of optical elements. The results reveal that the ellipsometric configuration with speed ratio 1:1 is preferred over the other configurations. Moreover, the angle that the fast axis of the retarder makes with the p polarization is found to have a crucial impact on the results. On the other hand, a small misalignment of the optical elements does not have a considerable impact on the results.

References

[1] Azzam R M and Bashara N M 1977 *Ellipsometry and Polarized Light* (Amsterdam: North-Holland)

[2] Kim Y T, Collins R W and Vedam K 1990 *Surf. Sci.* **233** 341

[3] Aspnes D E 2004 *Thin Solid Films* **455** 3

[4] El-Agez T M, El Tayyan A A and Taya S A 2010 *Thin Solid Films* **518** 5610

[5] El-Agez T M, Wieliczka D M, Moffitt C and Taya S A 2011 *Journal of Atomic, Molecular, and Optical Physics* **295304** 6

[6] Aspnes D E 1973 *Opt. Commun.* **8** 222

[7] Chen L Y, Feng X W, Su Y, Ma H Z and Qian Y H 1994 *Appl. Opt.* **33** 1299

[8] An I, Park M, Bang K, Oh H and Kim H 2002 *Jpn. J. Appl. Phys.* **41** 3978

[9] El-Agez T M and Taya S A 2010 *Journal of Sensors* **706829** 7

[10] El-Agez T M and Taya S A 2011 *Physica Scripta* **025701** 7

[11] El-Agez T and Taya S A 2011 *Opt. Lasers Eng.* **49** 507

[12] El-Agez T M, Wieliczka D M, Moffitt C and Taya S A 2011 *Physica Scripta* **045302** 5

[13] El-Agez T, Taya S A and El Tayayn A 2011 *Int. J. Optomechatronics* **5** 51

[14] Taya S A and El-Agez T M 2011 *Journal of Electromagnetic Analysis and Applications* **3** 351

[15] Fujiwara H 2007 *Spectroscopic Ellipsometry Principles and Applications* (West Sussex: John Wiley & Sons)

[16] Palik E D 1985 *Handbook of Optical Constants of Solids* (San Diego: Academic Press)

[17] Taya S A and El-Agez T M 2012 *Physica Scripta* **045706** 6